

Observing Spin Correlations in Single Top Production and Decay

Gregory Mahlon*

Department of Physics, McGill University, 3600 University St., Montréal, QC H3A 2T8, Canada
Electronic address: mahlon@physics.mcgill.ca

The weak decay of a polarized top quark has a rich structure of angular correlations among its decay products. We describe some of the noteworthy features of such decays. We then examine the three modes of single top production, with an emphasis on the status of calculations of the degree and direction of polarization at Run II of the Tevatron. The associated production of a top quark with a W boson will be very difficult to observe at the Tevatron. Prospects for observing the other two production mechanisms are much better. The spin state of the produced top quark is understood at leading order in the W^* production channel. For the Wg -fusion process, we present new results including the resummed logarithmic corrections of the form $\ln(m_t^2/m_b^2)$. The spin-dependence of the complete order α_s corrections to either of these processes has not yet been determined. The fraction of spin up top quarks is large ($\gtrsim 95\%$) for both modes provided that the appropriate spin quantization axis is chosen. McGill/00-33

1 Introduction

One of the major physics goals of Run II at the Fermilab Tevatron will be to study the top quark in as much detail as possible. The anticipated large data sets (2 fb^{-1} in Run IIa and as much as 15 fb^{-1} in Run IIb) will allow for refined measurements of the top quark mass and production cross sections. In addition to $t\bar{t}$ pairs, single t quarks are expected to be produced in great enough numbers to allow for their observation and a direct measurement of $|V_{tb}|$. Furthermore, it will be possible to study the kinematic and angular distributions associated with various top quark production and decay channels.

A unique feature of single top production is the large net polarization ($\gtrsim 95\%$) for the appropriate choice of spin quantization axis.¹ The top quark provides the only laboratory in which we can study the properties of an isolated quark: the large value of m_t implies that its weak decay will take place before the strong interaction can affect its spin.² Studies of the spin-induced angular

correlations among the top quark decay products are possible in both the $t\bar{t}$ and single t production modes. Although $t\bar{t}$ pairs will be produced in greater numbers than single tops, the relative simplicity of the final state in the single top case may compensate for the smaller statistics. In particular, with only one top quark to reconstruct, the combinatoric background for single t should be smaller than for $t\bar{t}$. Furthermore, as we shall see below, events where the W boson decays leptonically have the most distinctive correlations. Thus, the largest correlations in $t\bar{t}$ events occur when the kinematics are the most difficult to constrain because of a pair of invisible neutrinos. This reconstruction ambiguity is less severe in single top events, where there is just one neutrino.

2 Polarized Top Decay

Within the Standard Model, the dominant decay chain of the top quark is

$$t \longrightarrow W^+ b \quad \left\{ \begin{array}{l} l^+ \nu \\ \bar{d} u \end{array} \right. \quad (1)$$

Because of the parity-violating $V - A$ structure of the couplings to the W boson, the decay products of a polarized top quark possess a rich structure of angular correlations. For concreteness, we will describe the leptonic W decay. However, everything which we say about the charged lepton applies equally to the d -type quark when the W decays hadronically.

The simplest set of correlations are most-easily understood in the top quark rest frame, where we define χ_i^t to be the angle between the i th decay product and the top quark spin quantization axis (see Fig. 1). The decay angular distributions are simply linear in the cosine of these decay angles:³

$$\frac{1}{\Gamma_T} \frac{d\Gamma}{d(\cos \chi_i^t)} = \frac{1}{2} (1 + \alpha_i \cos \chi_i^t). \quad (2)$$

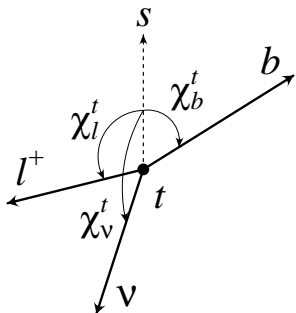


Figure 1: Definition of the top quark decay angles in the top quark rest frame. The direction of the top quark spin is indicated by the vector s . For simplicity, we have omitted the W boson and its decay angle $\chi_W^t \equiv \pi - \chi_b^t$. Although we have drawn this figure assuming a leptonic W decay, the same correlations hold in a hadronic decay if we replace the charged lepton by the d -type quark and the neutrino by the u -type quark.

Table 1: Correlation coefficients α_i for both semileptonic and hadronic top quark decays.^{3,4} The first two entries are a function of m_i^2/m_W^2 , and have been evaluated using the PDG2000 average values⁵ $m_t = 174.3 \pm 5.1$ GeV and $m_W = 80.419 \pm 0.056$ GeV.

Decay Product	α_i
W	0.403 ± 0.025
b	-0.403 ± 0.025
$\nu_\ell, u, \text{ or } c$	-0.324 ± 0.040
$\bar{\ell}, \bar{d}, \text{ or } \bar{s}$	1.000 (exactly)

Eq. (2) applies to spin up t quarks as well as to spin down \bar{t} quarks. The analyzing power α_i encodes the degree to which each decay product is correlated with the spin of the parent top quark. Table 1 lists the values of the α_i 's for each of the top quark decay products. The corresponding angular distributions are plotted in Fig. 2.

According to Table 1, the charged lepton is maximally correlated with the t spin direction, $\alpha_\ell = 1$, independent of the t and W masses. Amusingly, the charged lepton possesses a stronger correlation than its parent, the W boson. The resolution to this minor mystery lies in the significant interference between the polarization states of the intermediate W boson.⁶ It is well-known that the W bosons emitted from decaying top quarks have a specific mixture of helicities^a in the Standard Model: the right-handed helicity state is absent, while the left-handed and longitudinal states are present in the ratio $2m_W^2 : m_t^2$ (see Eq. (3) below). In Fig. 3 we have replotted the distribution of the charged lepton in the top quark rest frame, along with the results that would be obtained either by including only left-handed or longitudinal W 's. By comparing these distributions we see that there is complete destructive interference between the two W polarization states when the charged lepton is emitted antiparallel to the t spin. In the forward direction, however, there is a large degree of constructive interference. Thus, not all of the information about the t spin possessed by the W bosons is reflected by their distribution in $\cos \chi_W^t$: additional information is contained in the $W_{\text{left}}-W_{\text{long}}$ interference terms, and that information is imparted to the charged lepton, endowing it with its maximal analyzing power. For a spin down top quark, all of the correlations are reversed, as is the sign of the interference term. In fact, in the sum over the two top quark spins, the interference term exactly cancels point-by-point in phase space. Thus, for an unpolarized sample of top quarks the interference term plays no role in the charged lepton distribution.

^aIt turns out that the helicity basis is the only spin basis in which just two of the three spin states contribute. Hence, it is the most natural basis for discussing the W spin in top quark decays.

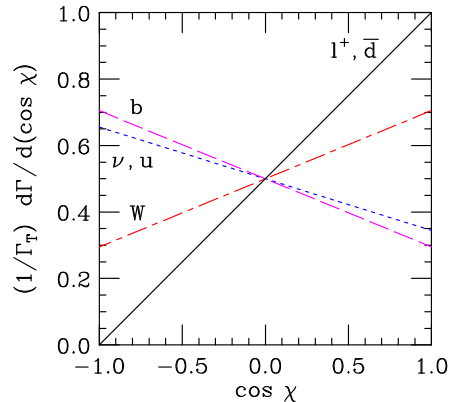


Figure 2: Angular correlations in the decay of a spin up top quark. The lines labeled ℓ^+ , \bar{d} , b , ν , u , and W describe the angle between the spin axis and the particle in the rest frame of the top quark.

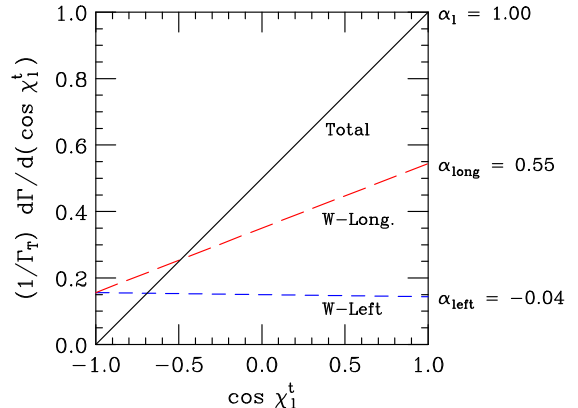


Figure 3: Angular distribution of the charged lepton in the top quark rest frame, assuming that only left-handed or longitudinal W bosons appear in the intermediate state. The relative areas under these two lines reflects the ratio of left-handed to longitudinal W bosons in t decay. The solid line is the quantum mechanical sum of the two contributions, and exhibits constructive (total destructive) interference when the lepton is emitted parallel (antiparallel) to the t spin.⁶

The distribution of the two helicity states of the W , as viewed in the top rest frame is not uniform, but may be intuitively understood from elementary angular momentum conservation arguments and the $V-A$ coupling between the W and quarks. Since the mass of the b quark is much smaller than the energy imparted to it from the decay, the left-handed chirality of the tbW vertex translates into a left-handed helicity for the b . Suppose first that the W boson is emitted along the top quark spin axis, as in Fig. 4a. Then, the spin of the b points in the same direction as the spin of the original t and we must have zero spin projection for the W boson (*i.e.* it must be longitudinal). On the other hand, when the W is emitted in the backwards direction (Fig. 4b), the spin of the b is opposite to the spin of the parent t . In this case, the W must have left-handed helicity in order to

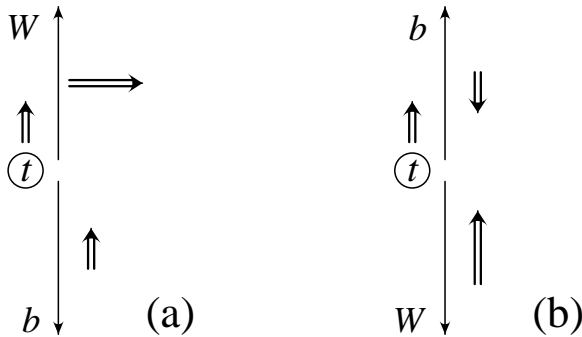


Figure 4: Angular momentum conservation in the decay of a polarized top quark. Since the b quark is effectively massless and couples to a W , it is produced with left-handed helicity. (a) W bosons emitted parallel to the top quark spin are longitudinal. (b) W bosons emitted antiparallel to the top quark spin are left-handed.

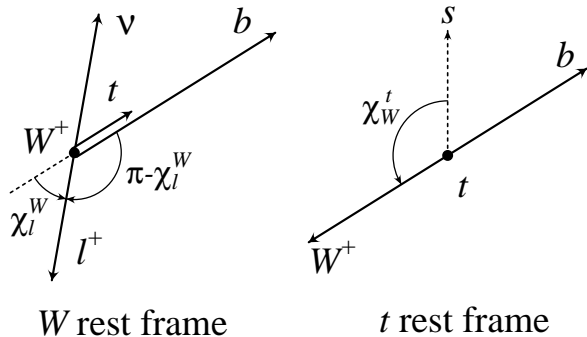


Figure 5: Definition of the W decay angles in top quark decay. We define $\pi - \chi_\ell^W$ to be the angle between the b quark direction and the charged lepton direction in the W rest frame. The other interesting angle is χ_W^t , the angle between the W boson momentum and the top quark spin axis in the top quark rest frame.

conserve angular momentum.

Because the left-handed and longitudinal W 's are emitted preferentially in different directions in the top quark rest frame, there is an interesting correlation between this angle (χ_W^t) and the emission angle (χ_ℓ^W) of the charged lepton as viewed in the W rest frame (see Fig. 5). This correlation is displayed in Fig. 6, where the dashed lines indicate the distribution at tree level⁷ and the solid lines show the consequences of including the $\mathcal{O}(\alpha_s)$ corrections to the decay matrix element.⁸ Inclusion of the NLO QCD corrections does not greatly modify the distribution: the features we expected from our intuitive argument are still clearly visible. In particular, the W 's which are emitted in the forward direction relative to the top spin show the characteristic $\sin^2 \chi_\ell^W$ associated with their longitudinal polarization, whereas the backwards-going W 's display the $\frac{1}{2}(1 - \cos \chi_\ell^W)^2$ distribution associated with their left-handed helicity. Even if sufficient statistics to map out the complete double differential distribution are not available, it may still be possible to test

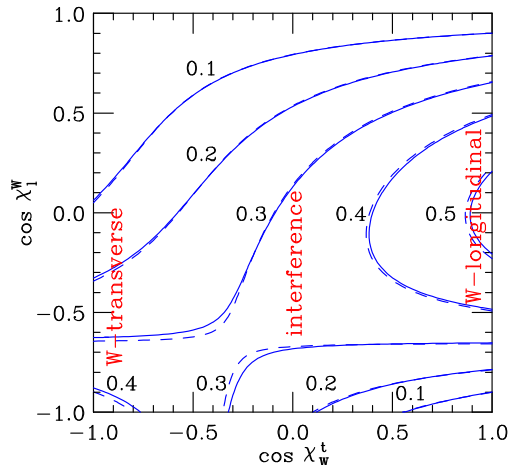


Figure 6: Contours of the decay distribution of a spin up top quark in the $\cos \chi_W^t$ - $\cos \chi_\ell^W$ plane. W bosons emitted in the forward direction ($\cos \chi_W^t \sim 1$) are primarily longitudinal, while backward-emitted W 's are mostly transverse. Interference between the two spin orientations dominates in the region around $\cos \chi_W^t = 0$. The dashed lines indicate the distribution at tree level.⁷ The solid lines are the distribution including the $\mathcal{O}(\alpha_s)$ corrections.⁸

this prediction. In Fig. 7 we divide the charged leptons into two groups according to the direction of the parent W , and plot the resulting distributions versus $\cos \chi_\ell^W$.^b The two samples clearly display differing distributions, reflecting the correlation between the emission angle of the W boson and its helicity. Of course, if we integrate the double differential distribution plotted in Fig. 6 over all values of χ_W^t , we obtain the famous result for the distribution of the charged lepton in the W rest frame

$$\frac{1}{\Gamma_T} \frac{d\Gamma}{d(\cos \chi_\ell^W)} = \frac{3}{4} \frac{m_t^2 \sin^2 \chi_\ell^W + 2m_W^2 \frac{1}{2}(1 - \cos \chi_\ell^W)^2}{m_t^2 + 2m_W^2}, \quad (3)$$

which is plotted as the solid curve in Fig. 7. Note that the distribution in Eq. (3) also applies to the decay of unpolarized top quarks, although the correlation between W polarization state and emission angle illustrated in Figs. 3 and 6 disappears in that case.

3 Single Top Production

Having described the features of the decays of polarized top quarks, we now address the question of how to produce polarized top quarks in the first place. The answer is simple: look at events containing single top quarks. Within the Standard Model, there are three distinct channels for the production of single tops, which we will now examine.

^bIn Fig. 7 we have arbitrarily chosen our cut point to be at $\cos \chi_\ell^W = \pm 0.5$. The optimal cut point for defining these two samples should be determined from a detailed study including backgrounds and detector effects.

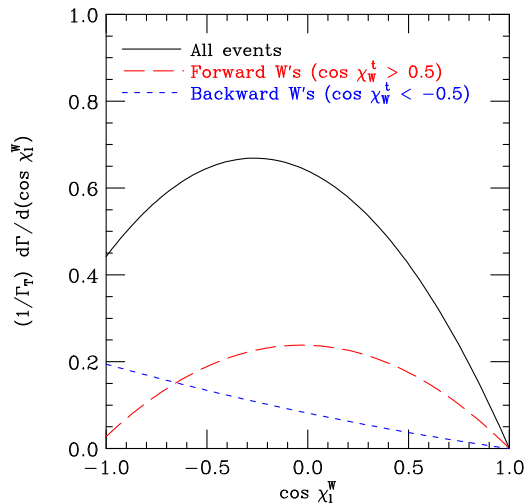


Figure 7: Charged lepton angular distributions in the W rest frame associated with the decay of a spin up top quark. Compared are samples selected on the basis of the emission angle of the W boson in the top quark rest frame.

We begin our survey with associated production,^{9–12} where the top quark is produced in conjunction with a W boson. The lowest order graphs for this process are illustrated in Fig. 8. Because this is a sea-sea process, the sum of t and \bar{t} production cross sections is only of order 0.1 pb for $p\bar{p}$ collisions at $\sqrt{s} = 2$ TeV. This small production cross section when coupled to the large insidious background from $t\bar{t}$ production will make this process very difficult to observe at Run II.¹¹ The prospects for the observation of this channel are brighter at the LHC.¹³ However, we have been unable to construct a spin basis in which the tops in this channel are produced with a high degree of polarization, limiting the potential usefulness of this mode for the study of angular correlations.

The second-largest mode of single top production at the Tevatron is predicted to be the W^* or s -channel production mechanism^{14–17} (see Fig. 9). Conceptually, this is a very simple process: a u quark and a \bar{d} quark annihilate, forming an off-shell W which “decays” to a t quark

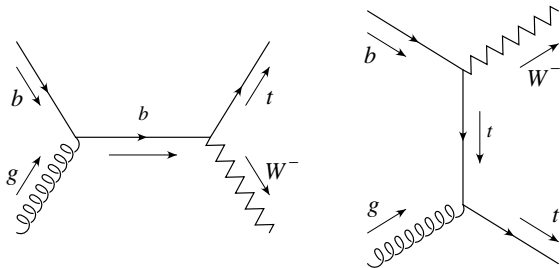


Figure 8: Leading order Feynman diagrams for tW^- associated production.

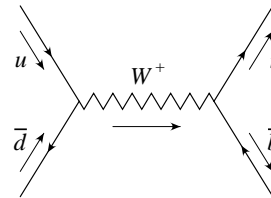


Figure 9: Leading order Feynman diagram for single top quark production in the W^* process.

and a \bar{b} quark. Crossing symmetry trivially relates this diagram to the one for top decay followed by a hadronic W decay. Given that the d -type quark is maximally correlated with the top quark spin, it follows that in the production process, the top quark is 100% polarized in the direction of the d -type quark.¹ Since the proton beam is a copious source of quarks and the antiproton beam a copious source of antiquarks, we intuitively expect that the d -type quark will come from the antiproton beam most of the time. In fact, we find that the antiproton beam supplies the d -type quark more than 97% of the time at a center of mass energy $\sqrt{s} = 2.0$ TeV (see Table 2). Thus, we define the *antiproton basis* to be that basis where the top quark spin is measured along the direction of the antiproton beam momentum.¹ For comparison, we also consider results in the more traditional helicity basis. Since helicity is a frame-dependent concept for massive particles, the result depends on whether we use the top quark direction in the lab frame or zero momentum frame (ZMF) to define the helicity. The spin contents in these three bases (lab helicity, ZMF helicity, and antiproton) are listed in Table 3. The third column of this table contains the spin asymmetry

$$\mathcal{A}_{\uparrow\downarrow} \equiv \frac{N_{\uparrow} - N_{\downarrow}}{N_{\uparrow} + N_{\downarrow}}. \quad (4)$$

This quantity governs the size of the observable angular correlations: in a situation where a mixture of spin up and spin down top quarks is present, Eq. (2) becomes

$$\frac{1}{\Gamma_T} \frac{d\Gamma}{d(\cos \chi_i^t)} = \frac{1}{2} \left(1 + \mathcal{A}_{\uparrow\downarrow} \alpha_i \cos \chi_i^t \right). \quad (5)$$

From Table 3 we see that the correlations are predicted to be larger in the antiproton basis by a factor of 1.7 over the lab frame helicity basis and by a factor of nearly 1.5 over the ZMF helicity basis. Thus, the antiproton basis provides a significantly better handle on the top quark spin than either of the two naturally-defined helicity bases.

The $\mathcal{O}(\alpha_s)$ corrections to the total rate for the W^* process have been computed by Smith and Willenbrock.¹⁷ They are large, increasing the sum of the t and \bar{t} production cross sections from 0.59 pb to 0.88 pb (+54%) for

Table 2: Fractional cross sections at leading order for single top quark production in the W^* channel at the Tevatron with $\sqrt{s} = 2.0$ TeV, decomposed according to the parton content of the initial state.¹⁸

p	\bar{p}	Fraction
u	\bar{d}	97 %
\bar{d}	u	2 %
c	\bar{s}	0.5%
\bar{s}	c	0.5%

Table 3: Dominant spin fractions and asymmetries at leading order for single top quark production in the W^* channel at the Tevatron with $\sqrt{s} = 2.0$ TeV.¹⁸

Basis	Spin Content	$\mathcal{A}_{\uparrow\downarrow}$
LAB helicity	78% L	-0.56
ZMF helicity	83% L	-0.65
antiproton	98% \uparrow	+0.96

the Tevatron at 2 TeV. Clearly a calculation of this correction including the full top quark spin dependence is desirable to verify that the large top quark spin asymmetry in the antiproton basis continues to hold.

The third, and, in fact, dominant production mechanism for single top quarks at the Tevatron at 2.0 TeV is the so-called W -gluon fusion process,^{19–29} also referred to as the t -channel process. At next-to-leading order, the sum of the t and \bar{t} cross sections in this mode is 2.12 ± 0.10 pb.³⁰ The lowest-order treatment of the spin correlations in these events is based upon the two pairs of diagrams illustrated in Fig. 10.¹ In these diagrams, a gluon from one beam splits into a $b\bar{b}$ or $t\bar{t}$ pair, which fuses with a W radiated from a light (u or \bar{d}) spectator quark from the other beam. The final state contains a (relatively low- p_T) \bar{b} jet, the top quark decay products, and the spectator jet.

The production of top quarks whose spin is *anti-aligned* with the direction of the d -type quark proceeds entirely through diagrams (b) and (d), where the gluon splits into a $t\bar{t}$ pair. On the other hand, top quarks whose spin is aligned with the d -type quark directions come from all four diagrams. Diagrams (a) and (c) are divergent as $m_b \rightarrow 0$, and dominate the lowest-order result for $m_b \ll m_t$. Hence, the top quark spin is highly correlated with the direction of the d -type quark, being aligned with this axis 97% of the time.¹

Of course, it is not possible in any given event to know where the d -type quark is with certainty. In fact, the d -type quark could be contained in either beam or in the spectator jet. We know that the u quark content of the proton is greater than the \bar{d} quark content of the

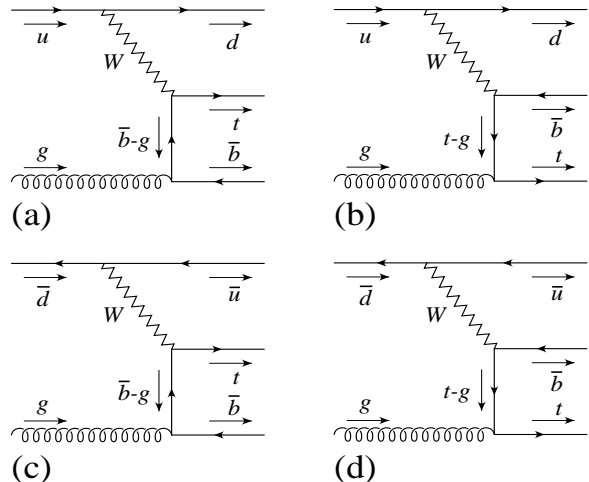


Figure 10: Gauge-invariant set of Feynman diagrams for single top quark production via Wg -fusion. The lower two diagrams are related to the upper two diagrams by crossing symmetry.

Table 4: Fractional cross sections for single top quark production in the Wg -fusion channel at the Tevatron with $\sqrt{s} = 2.0$ TeV, decomposed according to the parton content of the initial state¹⁸ ($2 \rightarrow 3$ diagrams only).

p	\bar{p}	Fraction
u	g	67%
g	u	3%
c	g	1%
g	c	1%
g	\bar{d}	21%
\bar{d}	g	3%
g	\bar{s}	2%
\bar{s}	g	2%

antiproton. Furthermore, the gluon content of both is the same. Hence, we expect that the largest share of the cross section comes from $ug \rightarrow t\bar{b}d$, with the spectator jet containing the d quark. As we can see from Table 4, this expectation is correct. In fact, the spectator jet contains the d -type quark approximately three-quarters of the time. Furthermore, in those events where the d -type quark is in the initial state, the fact that the spectator jet tends to be produced in the forward direction means that it is still not a bad choice for the spin quantization axis: it is “almost” in the ideal direction. Thus, we define the *spectator basis* as the basis in which we choose the spin axis to be aligned with the momentum of the spectator jet.¹ In this basis, the top quark is produced in the spin up state 95% of the time at leading order (see Table 5).

The situation at next-to-leading order is somewhat

Table 5: Dominant spin fractions and asymmetries for single top quark production in the Wg -fusion channel at the Tevatron with $\sqrt{s} = 2.0$ TeV.¹⁸ Compared are the leading order result ($2 \rightarrow 3$ diagrams only) and the leading order plus resummed large logs result (the contributions represented in Fig. 11).

Basis	2→3	only	LO+large logs	
	Spins	$\mathcal{A}_{\uparrow\downarrow}$	Spins	$\mathcal{A}_{\uparrow\downarrow}$
LAB helicity	64% L	-0.28	68% L	-0.36
ZMF helicity	83% L	-0.65	undefined	
spectator	95% \uparrow	+0.90	96% \uparrow	+0.93

complicated. The divergence of diagrams (a) and (c) as $m_b \rightarrow 0$ leads to large logarithms of the form $\ln(m_t^2/m_b^2)$. Because these logarithms convert the perturbation series from an expansion in α_s to one in $\alpha_s \ln(m_t^2/m_b^2)$, it is desirable to resum these logs by introducing a parton distribution function for the b quark.^{29,31–33} Once we have done this, the leading-order diagrams are for the $2 \rightarrow 2$ process represented in Fig. 11a. The original $2 \rightarrow 3$ process (Fig. 11c) becomes subleading. Because the logarithmic portion of the $2 \rightarrow 3$ process is already included in the b quark PDF used to compute the $2 \rightarrow 2$ process, it is necessary to subtract the overlapping portion of these two diagrams to avoid double counting (Fig. 11b). The combination of the three diagrams in Fig. 11 may be described as “leading order plus resummed large logs.” To complete the full NLO computation, we must add in the “true” α_s corrections coming from loops and soft parton radiation.

The spin structure of the three diagrams in Fig. 11 is understood.³⁴ The $2 \rightarrow 3$ diagrams give precisely the same contributions as were described above: the top quark spin is aligned with the d -type quark 97% of the time. The $2 \rightarrow 2$ diagram, being a crossed version of t decay, produces tops whose spin is aligned with the d -type quark 100% of the time. Because the overlap piece is to be evaluated with the intermediate b quark on-shell, the overlap term also has the same spin structure as the $2 \rightarrow 2$ piece. As a consequence of considering the next-to-leading order process, it becomes impossible to unambiguously define what is meant by the ZMF helicity basis, even theoretically. That is, should we take the ZMF of the initial state or the ZMF of the final state? Experimental considerations do not resolve this ambiguity, since on one hand we cannot directly measure the momentum fractions of the incoming partons, and on the other hand the \bar{b} quark is hard to see. Thus, in reality, there are only two viable choices for the spin basis: the lab frame helicity basis and the spectator basis. As we can see from the final two columns of Table 5, the spectator basis is superior to the lab frame helicity basis, producing corre-

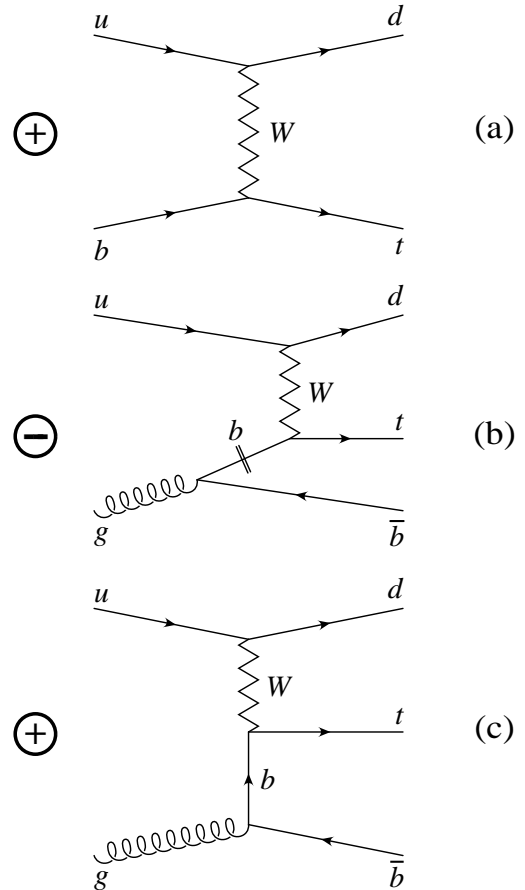


Figure 11: Representative Feynman diagrams for the leading order plus resummed large logs computation of single top quark production via Wg -fusion. The middle diagram represents the overlap between the $2 \rightarrow 2$ and $2 \rightarrow 3$ processes which results when the powers of $\ln(m_t^2/m_b^2)$ are resummed and absorbed into the b -quark parton distribution function.

lations which are larger by a factor of 2.6. Not included in Table 5 is the effect of the “true” $\mathcal{O}(\alpha_s)$ corrections, since their spin dependence has not yet been computed. These corrections shift the total cross section by approximately 12%.²⁹

4 Observing Correlations

We now briefly address the question of actually trying to observe these correlations in a collider environment such as the Tevatron.^c Consider single top quarks generated by the Wg -fusion process. We know that if the direction of the spectator jet is chosen as the spin quantization axis, then $\mathcal{A}_{\uparrow\downarrow} = 0.93$. Furthermore, if we choose those events where the W boson decays leptonically, then the charged lepton has the strongest correlation with the top quark spin, $\alpha_\ell = 1$. Hence, the most distinctive correla-

^cStudies of the situation at the LHC appear in Sec. 5.4 of Ref. 13.

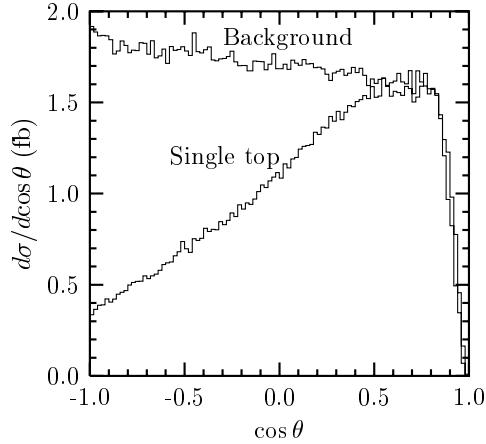


Figure 12: Monte Carlo results of Stelzer, *et al.*³⁵, for the top quark rest frame angular distribution of the charged lepton in single top quark events at the Tevatron ($\sqrt{s} = 2$ TeV), with respect to the untagged jet. Also shown is the angular distribution of the background events passing their selection criteria.

tions appear when we measure the angle χ_ℓ^t between the spectator jet and the charged lepton in the rest frame of the top quark.

Stelzer *et al.* have performed a first study of how well this measurement can be performed at the Tevatron.³⁵ They simulate the Wg -fusion process at 2 TeV including backgrounds and the effects of energy smearing, jet reconstruction, and cuts (for complete details, see Ref. 35). Their data set for the study of spin correlations consists of events where there is exactly one b -tagged and one untagged jet with a transverse momentum above 20 GeV. These cuts help to control the background from $t\bar{t}$. The untagged jet is assumed to be the spectator jet. The top quark rest frame is reconstructed by selecting the solution for the neutrino momentum with the smallest magnitude of rapidity. Using these assumptions, they plot the distribution in the angle θ , which is the angle between the charged lepton and the untagged jet in the reconstructed top quark rest frame. This angle is their best approximation to the theoretical angle χ_ℓ^t . Their results are shown in Fig. 12. The bins near $\cos\theta = 1$ are depleted by the isolation cut imposed on the lepton to distinguish it from the spectator jet. Away from this region, the signal shows a distinct slope, while the background is nearly flat.

To quantify the size of the correlations present in Fig. 12, Stelzer *et al.* define a cross section asymmetry over the range $-1 \leq \cos\theta \leq 0.8$, excluding the region where the cuts are most troublesome. Specifically,

$$A \equiv \frac{\sigma(-1 \leq \cos\theta \leq -0.1) - \sigma(-0.1 \leq \cos\theta \leq 0.8)}{\sigma(-1 \leq \cos\theta \leq -0.1) + \sigma(-0.1 \leq \cos\theta \leq 0.8)}. \quad (6)$$

In the ideal case where we assume that we correctly identify the spectator jet 100% of the time and measure all

momenta and angles (including those associated with the neutrino) perfectly, then we would obtain $A = -45\%$. The authors of Ref. 35 report that for the signal distribution in Fig. 12, $A = -38\%$. The difference is attributable to the effects of cuts, smearing, and the use of θ instead of χ_ℓ^t . Of course, what would be measured in a real experiment is the sum of the signal and background distributions, in which case A is further reduced to -14% . Nevertheless, with the 2 fb^{-1} of integrated luminosity expected at Run IIa, this asymmetry should be visible at the 3σ level.³⁵ The 5σ level requires a total of 5 fb^{-1} , which should be easily reached by Run IIb.

5 Summary

The Standard Model weak decays of polarized top quarks have a rich structure of angular correlations induced by the $V - A$ structure of the Wtb vertex. The charged lepton or d -type quark from the decaying W boson is maximally correlated with the spin of the parent top quark. Interference between the left-handed and longitudinal W bosons plays a crucial role in producing this correlation. The emission angle of the W boson with respect to the top quark spin is correlated with its polarization state. Longitudinal (left-handed) W bosons are emitted primarily parallel (antiparallel) to the direction of the top quark spin in its rest frame.

Single top production provides a source of polarized top quarks. With the exception of the associated production mode (which is too small to observe at the Tevatron), single top quarks are produced with a large degree of polarization when the appropriate spin basis is chosen. In the antiproton basis, 98% of the top quarks produced in the W^* channel have spin up. For Wg -fusion, 96% of the top quarks are produced with spin up in the spectator basis. The NLO corrections to the W^* mode are not known in a spin-dependent form. The portion of the higher order corrections which resums the large logarithms $\ln(m_t^2/m_b^2)$ are known including the spin dependence in the Wg -fusion case. They serve to increase the net polarization of the top quark by a small amount over the leading order result.

A recent study has shown for the Wg -fusion mode that the correlation between the top quark spin axis and the charged lepton should be observable at the 3σ level in Tevatron Run IIa. Additional studies are required to determine which of the other correlations associated with polarized top decay will be observable at the Tevatron.

Acknowledgments

Special thanks to the Thinkshop² organizers and especially the organizers of the Weak Interactions discussion group for a stimulating program. Thanks to Tim Stelzer,

Zack Sullivan, and Scott Willenbrock for the use of their figure from Ref. 35 in this talk.

High energy physics research at McGill University is supported in part by the Natural Sciences and Engineering Research Council of Canada and the Fonds pour la Formation de Chercheurs et l'Aide à la Recherche of Québec. I would also like to thank the Fermilab theory group for their hospitality and support during my visit.

References

- [*] Talk presented at the Thinkshop² on Top-Quark Physics for Run II, held at the Fermi National Accelerator Laboratory, November 10–12, 2000.
- [+] KEK-scanned preprints may be accessed at http://www-lib.kek.jp/cgi-bin/img_index?#, where the “#” should be replaced by the paper number.
1. G. Mahlon and S. Parke, Phys. Rev. **D55**, 7249 (1997), hep-ph/9611367.
 2. I. Bigi, Y. Dokshitzer, V. Khoze, J. Kühn, and P. Zerwas, Phys. Lett. **B181**, 157 (1986), KEK-8610194.
 3. M. Jeżabek and J.H. Kühn, Phys. Lett. **B329**, 317 (1994), hep-ph/9403366.
 4. A useful table of the complete t and W mass dependence of these coefficients is found in G. Mahlon and S. Parke, Phys. Rev. **D53**, 4886 (1996), hep-ph/9512264.
 5. D.E. Groom *et al.* (Particle Data Group), Eur. Phys. J. **C15**, 1 (2000), <http://pdg.lbl.gov>.
 6. G. Mahlon and S. Parke, in *Physics Potential and Development of Muon Colliders and Neutrino Factories*, edited by D.B. Cline, AIP Conference Proceedings **542**, 138 (2000), hep-ph/0001201.
 7. S. Parke and Y. Shadmi, Phys. Lett. **B387**, 199 (1996), hep-ph/9606419.
 8. M. Fischer, S. Groote, J.G. Körner, and M.C. Mauser, Phys. Lett. **B451**, 406 (1999), hep-ph/9811482.
 9. A.P. Heinson, A.S. Belyaev and E.E. Boos, Phys. Rev. **D56**, 3114 (1997), hep-ph/9612424.
 10. A.S. Belyaev, E.E. Boos and L.V. Dudko, Phys. Rev. **D59**, 075001 (1999), hep-ph/9806332.
 11. T. Tait, Phys. Rev. **D61**, 034001 (2000), hep-ph/9909352.
 12. A.S. Belyaev and E.E. Boos, “Single Top Quark $tW + X$ Production at the LHC: A Closer Look,” hep-ph/0003260.
 13. M. Meneke, I. Efthymiopoulos, M.L. Mangano, J. Womersley, *et al.*, hep-ph/0003033.
 14. S. Cortese and R. Petronzio, Phys. Lett. **B253**, 494 (1991).
 15. T. Stelzer and S. Willenbrock, Phys. Lett. **B357**, 125 (1995), hep-ph/9505433.
 16. R. Pittau, Phys. Lett. **B386**, 397 (1996), hep-ph/9603265.
 17. M.C. Smith and S. Willenbrock, Phys. Rev. **D54**, 6696 (1996), hep-ph/9604223.
 18. The values quoted in this table were obtained using the CTEQ5HQ parton distribution functions found in H.L. Lai, *et al.*, (CTEQ Collaboration), Eur. Phys. J. **C12**, 375 (2000), hep-ph/9903282. The spin fractions reported in this paper are not particularly sensitive to the choice of PDF, as may be verified by comparison to the results contained in Ref. 1, which utilizes an older PDF set.
 19. S. Dawson, Nucl. Phys. **B249**, 42 (1985), KEK-8407138.
 20. S. Willenbrock and D.A. Dicus, Phys. Rev. **D34**, 155 (1986), KEK-8603167.
 21. S. Dawson and S. Willenbrock, Nucl. Phys. **B284**, 449 (1987), KEK-8610370.
 22. C.-P. Yuan, Phys. Rev. **D41**, 42 (1990), KEK-8908225.
 23. R.K. Ellis and S. Parke, Phys. Rev. **D46**, 3785 (1992).
 24. G.V. Jikia, and S.R. Slabospitsky, Phys. Lett. **B295**, 136 (1992), KEK-9205163 (in Russian).
 25. F. Anselmo, B. van Eijk, and G. Bordes, Phys. Rev. **D45**, 2312 (1992), KEK-9112103.
 26. D.O. Carlson, and C.P. Yuan, Phys. Lett. **B306**, 386 (1993).
 27. G. Bordes and B. van Eijk, Z. Phys. **C57**, 81 (1993).
 28. G. Bordes and B. van Eijk, Nucl. Phys. **B435**, 23 (1995).
 29. T. Stelzer, Z. Sullivan, and S. Willenbrock, Phys. Rev. **D56**, 5919 (1997), hep-ph/9705398.
 30. Z. Sullivan, “A Theoretical Overview of Top Quarks and the Weak Interaction,” talk presented at the Thinkshop² on Top-Quark Physics for Run II, held at the Fermi National Accelerator Laboratory, November 10–12, 2000.
 31. F. Olness and W.-K. Tung, Nucl. Phys. **B308**, 813 (1988).
 32. R. Barrett, H. Haber, and D. Soper, Nucl. Phys. **B306**, 697 (1988).
 33. M. Aivazis, J. Collins, F. Olness, and W.-K. Tung, Phys. Rev. **D50**, 3102 (1994), hep-ph/9312319.
 34. G. Mahlon and S. Parke, Phys. Lett. **B476**, 323 (2000), hep-ph/9912458.
 35. T. Stelzer, Z. Sullivan and S. Willenbrock, Phys. Rev. **D58**, 094021 (1998), hep-ph/9807340.